iScience

CellPress
OPEN ACCESS

Article

Helicobacter pylori CagA promotes immune evasion of gastric cancer by upregulating PD-L1 level in exosomes

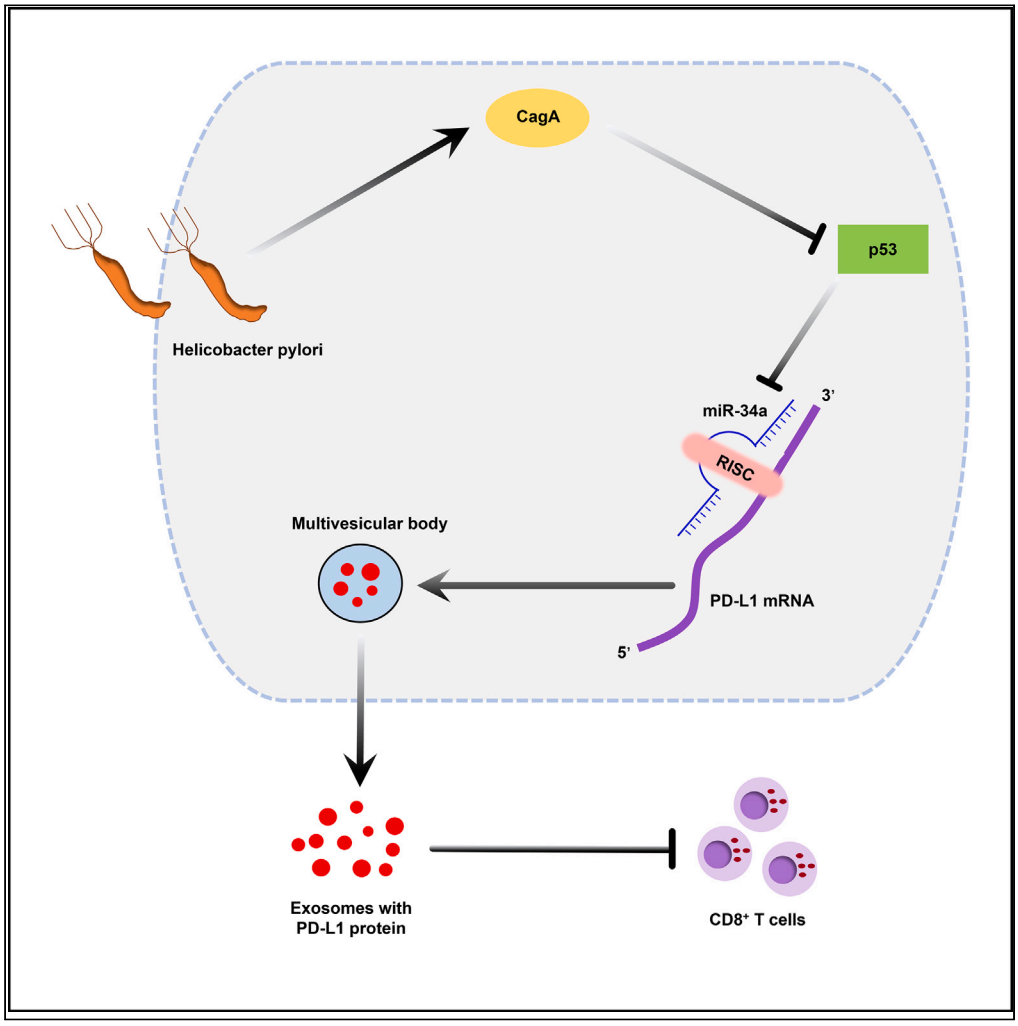

Jinfeng Wang, Rilin Deng, Shuai Chen, ..., Zhuo Chen, Haizhen Zhu, Chaohui Zuo

zuochaohui@vip.sina.com

Highlights

CagA increases exosomal PD-L1 level and promotes progression of Hp-infected GC

Exosomal PD-L1 inhibits proliferation and cytokine secretion of $CD8^+$ T cells

CagA promotes immune evasion of GC via regulating p53-*miR-34a*-PD-L1 signal axis

Wang et al., iScience *26*, 108414
December 15, 2023
https://doi.org/10.1016/j.isci.2023.108414

iScience

CellPress
OPEN ACCESS

Article

Helicobacter pylori CagA promotes immune evasion of gastric cancer by upregulating PD-L1 level in exosomes

Jinfeng Wang,[1] Rilin Deng,[2] Shuai Chen,[3] Shun Deng,[1] Qi Hu,[4] Biaoming Xu,[4] Junjun Li,[5] Zhuo He,[1] Mingjing Peng,[1] Sanlin Lei,[6] Tiexiang Ma,[7] Zhuo Chen,[8] Haizhen Zhu,[2] and Chaohui Zuo[1,3,4,9,*]

SUMMARY

Cytotoxin-associated gene A (CagA) of Helicobacter pylori (Hp) may promote immune evasion of Hp-infected gastric cancer (GC), but potential mechanisms are still under explored. In this study, the positive rates of CagA and PD-L1 protein in tumor tissues and the high level of exosomal PD-L1 protein in plasma exosomes were significantly associated with the elevated stages of tumor node metastasis (TNM) in Hp-infected GC. Moreover, the positive rate of CagA was positively correlated with the positive rate of PD-L1 in tumor tissues and the level of PD-L1 protein in plasma exosomes, and high level of exosomal PD-L1 might indicate poor prognosis of Hp-infected GC. Mechanically, CagA increased PD-L1 level in exosomes derived from GC cells by inhibiting p53 and *miRNA-34a*, suppressing proliferation and anticancer effect of $CD8^+$ T cells. This study provides sights for understanding immune evasion mediated by PD-L1. Targeting CagA and exosomal PD-L1 may improve immunotherapy efficacy of Hp-infected GC.

INTRODUCTION

Gastric cancer (GC) is a global health problem with high morbidity and high mortality.[1] Owing to cancer heterogeneity, the efficacy of conventional therapy represented by surgery, chemotherapy, radiotherapy is limited in clinic.[2] Chronic gastritis caused by Helicobacter pylori (Hp) infection is a major factor for suffering GC,[3–5] which may create an immunosuppressive microenvironment by regulating innate and adaptive immunity, resulting in host inability to eliminate infection. Although immunotherapy provides a way for improving the prognosis of malignances, the objective responsive rate and disease control rate of immune checkpoint blockades (ICBs) represented by anti-PD-1/PD-L1 antibodies for GC are only 12.0% and 34.7%.[6–8] To improve the therapeutic efficacy of ICBs, it is urgently needed to study the behand mechanisms of immune checkpoints in regulating the development and progression of GC.

Hp infection induces PD-L1 expression, which may cause immune evasion and poor prognosis of GC.[9,10] PD-L1 inhibits effective T cells via PD-1 engagement, promotes the development of regulatory T cells (Treg) from naive $CD4^+$ T cells and converts T-bet^+ Th1 cells into $FoxP3^+$ Treg cells, enhances tumor infiltration of myeloid-derived suppressor cells (MDSCs), leading to anti-PD-1/PD-L1 resistance.[11–13] In turn, immune imbalance caused by upregulated PD-L1 in Hp-infected GC cells favors bacterial persistence.[14] However, the regulatory mechanism of Hp infection on PD-L1 expression is not completely understood. Cytotoxin associated protein A (CagA) plays an important role in carcinogenesis of GC, functioning as an oncogenic factor to activate cancer signaling pathways.[15,16] Once entering into host cells, CagA may activate AKT and ERK to phosphorylate human double minute-2 (HDM2), causing the dissociation of HDM2-p53 protein complex and the activation of HDM2 and ARF-BP1 E3 protein ligase and thereby the rapid degradation of p53 protein.[17] Moreover, CagA may interact with the p53 apoptosis stimulating protein of p53-2 (ASPP2) to promote the degradation of p53 protein.[18] Interestingly, p53 negatively regulates PD-L1 expression by upregulating *miRNA-34a* (*miR-34a*) level in lung and cervical cancer.[19,20] Actually, *miR-34a* directly targets *PD-L1* 3′ UTR and inhibit PD-L1 surface expression in acute myeloid leukemia and cervical cancer.[20,21] Excepting for upregulating PD-L1 level, *miR-34a*

[1]Department of Gastroduodenal and Pancreatic Surgery, Translational Medicine Joint Research Center of Liver Cancer, Laboratory of Digestive Oncology, Hunan Cancer Hospital & The Affiliated Cancer Hospital of Xiangya School of Medicine, Central South University, Clinical Research Center For Tumor of Pancreaticobiliary Duodenal Junction In Hunan Province, Changsha 410013, Hunan, China
[2]Institute of Pathogen Biology and Immunology, College of Biology, State Key Laboratory of Chemo/Biosensing and Chemometrics, Hunan University, Changsha 410082, Hunan, China
[3]School of Integrated Traditional Chinese and Western Medicine, Hunan University of Traditional Chinese Medicine, Changsha 410208, Hunan, China
[4]Graduates School, University of South China, Hengyang 421001, Hunan, China
[5]Department of Pathology, Hunan Cancer Hospital & The Affiliated Cancer Hospital of Xiangya School of Medicine, Central South University, Changsha 410013, Hunan, China
[6]Department of General Surgery, The Second Xiangya Hospital of Central South University, Changsha 410011, Hunan, China
[7]The Third Department of General Surgery, The Central Hospital of Xiangtan City, Xiangtan 411100, Hunan, China
[8]Molecular Science and Biomedicine Laboratory (MBL), State Key Laboratory of Chemo/Biosensing and Chemometrics, College of Chemistry and Chemical Engineering, College of Biology, Aptamer Engineering Center of Hunan Province, Hunan University, Changsha 410082, Hunan, China
[9]Lead contact
*Correspondence: zuochaohui@vip.sina.com
https://doi.org/10.1016/j.isci.2023.108414

restoration may increase the recruitment of $CD8^+$ and $CD4^+$ T cells and suppresses the recruitment of macrophages and Tregs into tumor microenvironment in triple negative breast cancer.[22] Meanwhile, Epstein-Barr virus-encoded EBNA2 inhibits PD-L1 expression by downregulating *miR-34a* in B cell lymphomas.[23] However, evidence about the regulatory effect of CagA on p53-*miR-34a*-PD-L1 signal axis in Hp-infected GC is still unclear.

Exosomes are a group of extracellular vesicles with a diameter ranged from 30 nm to 200 nm, participating in cellular communication by transferring functional proteins, metabolites, and nucleic acids to recipient cells.[24–26] Exosomal PD-L1 retains immunosuppressive activity and is tightly associated with the poor prognosis of GC,[27,28] presenting a mechanism for explaining the immune evasion and immunosuppressive microenvironment of GC. CagA degrades p53 protein in a variety of ways, and the degradation of p53 protein may promote PD-L1 expression to trigger immune evasion of Hp-infected GC via exosomes. This study evaluated the prognostic value of exosomal PD-L1 and investigated the regulatory mechanism of CagA-p53-*miR-34a* signal axis on PD-L1 expression, exploring the immune evasion of Hp-infected GC. The findings in this study may provide sights for improving the efficacy of immunotherapy, especially for Hp-infected GC.

RESULTS

CagA expression is tightly associated with the high level of exosomal PD-L1 protein and the progression of Hp-infected GC

To determine the regulatory effect of CagA on exosomal PD-L1 in GC, tumor, and plasma specimens from a total of 87 GC patients infected with were collected for this study. CagA and PD-L1 proteins in tumor specimens were examined by immunohistochemistry (IHC) staining. It turned out that the positive rates of CagA and PD-L1 proteins in GC tissues were 71.3% and 54.0% (Figure 1A), respectively. Meanwhile, exosomes isolated from plasma of GC patients were characterized by transmission electron microscopy (TEM) and nanoparticle tracking analysis (NTA) (Figure 1B), which were further approved by examining the protein expression of specific markers including CD9, CD63, and TSG101 (Figure 1C). Interestingly, the level PD-L1 protein in exosomes derived from plasma of CagA positive GC was generally higher than that in CagA negative GC (Figure 1D). It seems that CagA might upregulate the protein level of exosomal PD-L1 in Hp-infected GC.

Next, Chi-square analyses showed that the positive rates of CagA and PD-L1 proteins in tumor tissues examined by IHC staining and the level of exosomal PD-L1 protein examined by western blot were significantly higher in GC patients characterized with T3-T4 stages, lymph node metastasis, and III-IV stages of tumor node metastasis (TNM) (Table 1). Besides, the positive rate of CagA was significantly associated with Lauren type GC with high positive rate in intestinal type GC (Table 1). Meanwhile, higher positive rate of PD-L1 protein in tumor tissues and higher level of PD-L1 protein in plasma exosomes were uncovered in undifferentiated and poor differentiated GC (Table 1). Thus, CagA and exosomal PD-L1 may promote the progression of Hp-infected GC. Moreover, CagA expression was positively correlated with the positive rate of PD-L1 protein in tumor tissues ($r = 0.332$, $p = 0.002$) and the level of PD-L1 protein in plasma exosomes ($\rho = 0.385$, $p < 0.001$) (Table 2), and the positive rate of PD-L1 protein in tumor tissues was positively correlated with the level of exosomal PD-L1 protein ($\rho = 0.828$, $p < 0.001$) (Table 2). These data suggested that CagA may promote malignant transformation and upregulate exosomal PD-L1 level in HP-infected GC.

Notably, low level of exosomal PD-L1 protein was found to improve the overall survival of Hp-infected GC ($p = 0.032$) (Figure 1E). By comparison, the lower level of PD-L1 protein in tumor tissues had no survival advantage for Hp-infected GC ($p = 0.212$) (Figure 1F). Thus, exosomal PD-L1 may be a prognosis factor in Hp-infected GC.

CagA promotes PD-L1 expression in GC

To explore the regulating mechanism of CagA on PD-L1 expression, eukaryotic expression plasmids of Flag-*CagA* was constructed and verified in HEK293T cells (Figure 2A). Then, *CagA* plasmids were transfected into human- and mouse-derived GC cells including AGS, HGC27, and MFC cells. It turned out that transfection of Flag-*CagA* upregulated the level of glycosylated PD-L1 protein and downregulated the level of p53 protein (Figure 2B). Interestingly, IHC staining showed that the positive rate of p53 was negatively correlated with the positive rate of PD-L1 in tumor tissues ($r = -0.375$, $p < 0.01$) and the level of PD-L1 protein in plasma exosomes of GC ($r = -0.496$, $p < 0.01$) (Figures 1A; Table 2), suggesting that p53 might be involved in the regulatory mechanism of CagA on exosomal PD-L1 expression. Interestingly, the level of glycosylated PD-L1 protein was downregulated by the increased level of p53 (Flag-*TP53* or Flag-*TrP53*) while upregulated by the decreased level of p53 (sh-*TP53* or sh-*TrP53*) in human- and mouse-derived GC cells (Figure 2C). However, the expression tendency of *miR-34a* was just opposite to that of PD-L1 in GC cells with different level of p53 (Figures 2C and 2D). Thus, p53 may promote *miR-34a* expression while inhibit PD-L1 expression in GC cells. We further evaluated the influence of *miR-34a* on PD-L1 expression. Compared with that of negative control (NC), the level of glycosylated PD-L1 protein on GC cells was downregulated by the transfection of *miR-34a* mimics (Figures 2E and 2F). These data suggested that CagA may promote PD-L1 expression through regulating signaling pathway mediated by p53 and *miR-34a*.

Exosomal PD-L1 protein may be upregulated by CagA

Next, we evaluated whether CagA might upregulate the level of PD-L1 protein in exosomes derived from GC cells. For this, exosomes in supernatants of cultured GC cells that transfected with Flag-*CagA* plasmids or control Flag-vector was isolated by ultracentrifugation. The size distribution and morphology of isolated exosomes were characterized by NTA and TEM (Figure 3A), and the expression of exosomal protein markers including CD9, CD63, and TSG101 were examined by western blot (Figure 3B), suggesting the successful isolation of exosomes derived from the supernatants of cell culture medium. Compared with that of Flag-vector group, the level of PD-L1 protein in exosomes that derived from the supernatants of cultured GC cells was upregulated by the transfection of Flag-*CagA* (Figure 3C). Thus, CagA promotes the expression of exosomal PD-L1, which may participate in the immune evasion of GC.

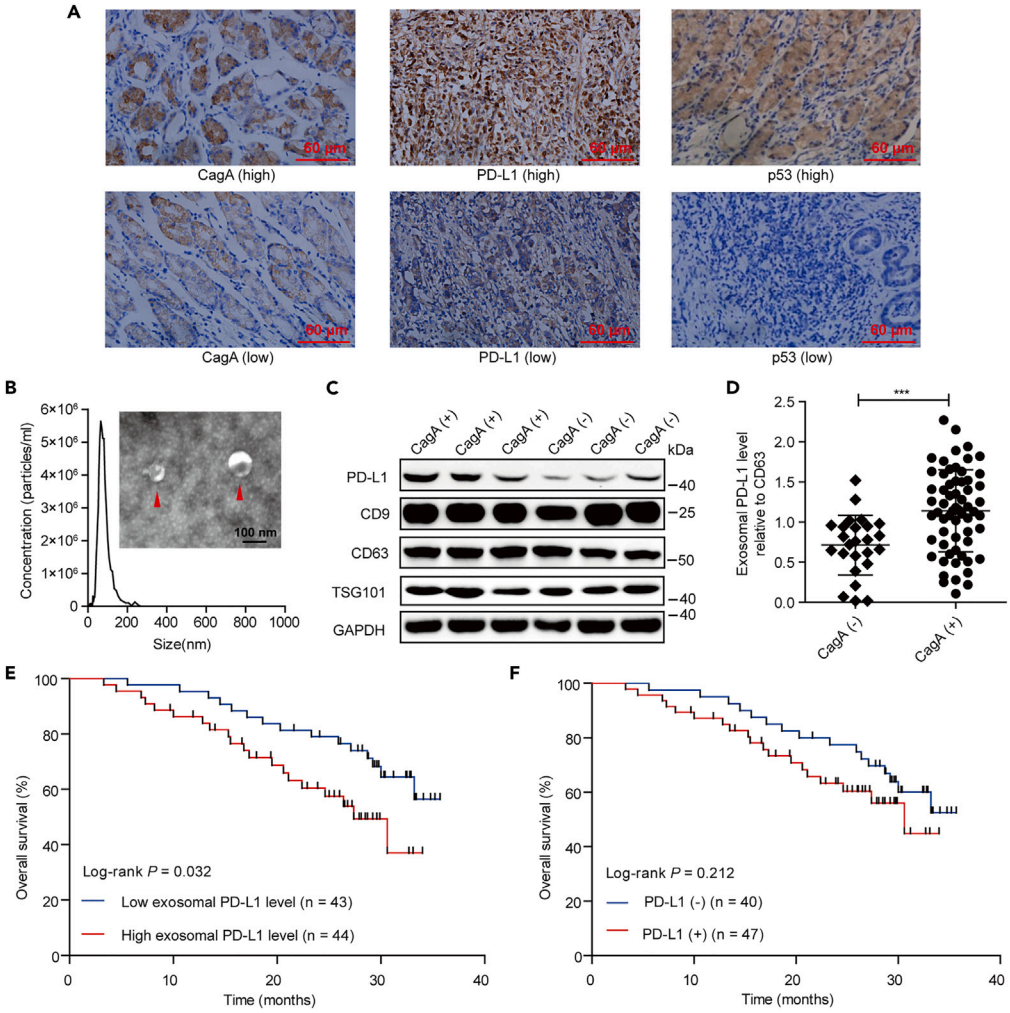

Figure 1. Regulatory effect of CagA expression on exosomal PD-L1 in Hp-infected GC

(A) IHC staining for protein levels of CagA, P53, and PD-L1 in representative tissue specimens of Hp-infected GC. Scale bar, 60 μm.

(B) NTA for size distribution and TEM for morphology of exosomes isolated from plasma of Hp-infected GC. Scale bar, 100 nm.

(C) Western blot for protein levels of PD-L1, TSG101, CD63, CD9, and PD-L1 in plasma exosomes derived from three representative CagA positive (+) and negative (–) GC patients.

(D) Scatterplots showing the relative level of PD-L1 protein in plasma exosomes of CagA positive (+) and negative (–) GC patients suffered from Hp infection. Data were analyzed by two-sided Student's t tests, and are represented as mean ± SD. ***p < 0.001.

(E and F) Kaplan-Meier analysis (log rank test) for overall prognosis of Hp-infected GC presenting high and low levels of PD-L1 protein in tumor tissues (E) and plasma exosomes (F).

PD-L1-enriched exosomes inhibits the proliferation and cytokine secretion of CD8$^+$ T cells

Immuno-oncology is mainly focused on T cell responses, especially for CD8$^+$ T cells. To figure out the influence of exosomal PD-L1 on immune evasion of GC, exosomes that derived from Flag-*CagA* or Flag-vector transfected AGS and HGC27 cells were blockaded with anti-PD-L1 (αPD-L1) or IgG and added into the culture medium of CD8$^+$ T cells that derived from peripheral blood of healthy individuals. Under the treatment of IgG, exosomes derived from CagA-expressed GC cells significantly inhibited the proliferation of human- and mouse-derived CD8$^+$ T cells (Figures 4A–4C). Meanwhile, the levels of secreted cytokines including IFN-γ, TNF-α, and IL-2 by CD8$^+$ T cells were significantly downregulated by the treatment of exosomes that derived from the *CagA*-transfected GC cells (Figures 4D–4F). Thus, the upregulated exosomal PD-L1 by CagA inhibits the proliferation and cytokine secretion of CD8$^+$ T cells. Notably, the inhibited proliferation of CD8$^+$ T cells and the downregulated levels of secreted cytokines by CD8$^+$ T cells caused by the treatment of exosomes derived from *CagA*-transfected GC cells was reversed by the treatment of αPD-L1 (Figures 4A–4F). PD-L1 blockade restores the proliferation and cytokine secretion of CD8$^+$ T cells that inhibited by CagA expression, being a promising method for improving the efficacy of immunotherapy for Hp-infected GC.

Table 1. Chi-square analyses for association between clinicopathological features and positive rates of CagA or PD-L1 protein expression or the level of exosomal PD-L1 protein in 87 Hp-infected GC

	Patients	CagA (+)		PD-L1 (+)		Exo PD-L1	
Clusters	Count (%)	Count (%)	*p*	Count (%)	*p*	Mean ± SD	*p*
Sex			0.850		0.720		0.709
Male	57 (65.5%)	41 (71.9%)		30 (52.6%)		1.00 ± 0.51	
Female	30 (34.5%)	21 (70.0%)		17 (56.7%)		1.05 ± 0.58	
Age			0.660		0.523		0.450
≤60	49 (56.3%)	34 (69.4%)		25 (51.0%)		1.05 ± 0.55	
>60	38 (43.7%)	28 (73.7%)		22 (57.9%)		0.97 ± 0.46	
Lauren type			0.025		0.489		0.375
Intestinal[a]	51 (58.6%)	41 (80.4%)		26 (51.0%)		1.06 ± 0.54	
Diffuse	36 (41.4%)	21 (58.3%)		21 (58.3%)		0.96 ± 0.46	
Differentiation type			0.360		0.022		0.023
Undifferentiated and poor	42 (48.3%)	28 (66.7%)		28 (66.7%)		1.15 ± 0.54	
Moderate and well	45 (51.7%)	34 (75.6%)		19 (42.2%)		0.90 ± 0.46	
Serum CEA			0.469		0.210		0.226
<5 ng/mL	54 (62.1%)	37 (68.5%)		32 (59.3%)		1.07 ± 0.54	
≥5 ng/mL	33 (37.9%)	25 (75.8%)		15 (45.5%)		0.93 ± 0.45	
Tumor diameter			0.711		0.097		0.078
≤5 cm	46 (52.9%)	32 (69.6%)		21 (45.7%)		0.93 ± 0.53	
>5 cm	41 (47.1%)	30 (73.2%)		26 (63.4%)		1.12 ± 0.48	
T stage			0.042		0.026		0.011
T1-T2	19 (21.8%)	10 (52.6%)		6 (31.6%)		0.76 ± 0.56	
T3-T4	68 (78.2%)	52 (76.5%)		41 (60.3%)		1.09 ± 0.48	
N stage			0.012		0.009		0.003
Negative	25 (28.7%)	13 (52.0%)		8 (32.0%)		0.76 ± 0.55	
Positive	62 (71.3%)	49 (79.0%)		39 (62.9%)		1.12 ± 0.46	
TNM stage			0.002		0.005		0.001
I-II	34 (39.1%)	18 (52.9%)		12 (35.3%)		0.79 ± 0.49	
III-IV	53 (60.1%)	44 (83.0%)		35 (66.0%)		1.16 ± 0.48	

[a]Intestinal type including intestinal, mixed, and other types.

Exosomal PD-L1 may promote the immune evasion of GC

The previous study suggested that high level of exosomal PD-L1 may drive the immune evasion of CagA-expressed GC cells by suppressing the proliferation and cytokine secretion of $CD8^+$ T cells. Here, *in vivo* experiments based on 615 mice and 615 mice-derived MFC cells were conducted to approve our findings. Compared with that of vector control, treatment of exosomes derived from *CagA*-transfected MFC cells promoted the growth of tumors formed by MFC cells (Figure 5A), which was statistically verified by the bigger size and heavier weight of tumors (Figures 5B and 5C). Thus, CagA expression and high level of exosomal PD-L1 may promote the development and progression of GC. Moreover, IHC staining showed that the level of PD-L1 protein in tumor tissues of mice in Flag-*CagA* group was higher than that in Flag-vector group (Figure 5D). However, the protein level of CD8 in these tumor tissues was just opposite with that of PD-L1 (Figure 5D). Thus, exosomes with high level of PD-L1 may enhance the immune evasion of Hp-infected GC.

DISCUSSION

PD-L1 is an important immune checkpoint with wide attention in multiple malignancies, but the association between PD-L1 expression and the prognosis of GC is still unsure at present. A meta-analysis showed that the positive rate of PD-L1 expression is ranged from 25% to 65% and tightly associated with the poor prognosis of GC.[29] However, clinical research with large samples shows that high level of PD-L1 may improve the survival rate of GC.[30] In this study, our IHC staining uncovered that PD-L1 expression in tumor tissues may be correlated with the poor survival of Hp-infected GC with no statistical significance ($p = 0.212$). Thus, PD-L1 expression in cancer tissues may be not a predictable biomarker for Hp-infected GC. Apart from PD-L1 expression in tumor tissues, cancer cells may secret PD-L1

Table 2. Correlation analysis among the positive rates of CagA, P53, PD-L1 protein expression in gastric cancer tissues and the level of exosomal PD-L1 protein in preoperative peripheral blood

	CagA				P53				PD-L1				Exo-PD-L1		
Clusters	–	+	r	P	–	+	r	P	–	+	r	P	Mean ± SD	ρ	P
CagA							−0.296	0.005			0.332	0.002		0.385	<0.001
–					8	17			18	7			0.71 ± 0.37		
+					40	22			22	40			1.14 ± 0.51		
P53			−0.296	0.005							−0.374	0.001		−0.496	<0.001
–	8	40							14	34			1.24 ± 0.39		
+	17	22							26	13			0.75 ± 0.52		
PD-L1			0.332	0.002			−0.374	0.001						0.828	<0.001
–	18	22			14	26							0.59 ± 0.29		
+	7	40			34	13							1.38 ± 0.34		

protein via exosomes to influence the malignant transformation and prognosis of cancer.[31,32] Notably, the Kaplan-Meier analysis of our study showed that high-level of exosomal PD-L1 protein was significantly associated with the poor prognosis of Hp-infected GC ($p = 0.032$). Hence, high level of PD-L1 protein in plasma exosomes may be a prognostic indicator for the development and progression of Hp-infected GC.

As an important mechanism of negative regulation on T cell activation to prevent autoimmune response under physiological conditions, PD-1 is highly expressed on active T cells.[33–35] However, the binding of PD-L1 concentrated on cancer cells to PD-1 on T cells may lead to immune evasion of malignant tumors.[36] In this study, PD-L1 in exosomes derived from *CagA*-transfected GC cells inhibited not only the proliferation and cytokine secretion (IFN-γ, TNF-α, and IL-2) of $CD8^+$ T cells *in vitro* but also the infiltration of $CD8^+$ T cells into the mouse tumors *in vivo*. Similar to that in non-small cell lung cancer,[37] exosomal PD-L1 may drive the immune evasion of Hp-infected GC. Moreover, this study uncovered that PD-L1 level in plasma exosomes is positively and highly correlated with the PD-L1 level in cancer tissues ($\rho = 0.828$, $p < 0.001$) in Hp-infected GC. So, excessive expression of PD-L1 protein may explain the poor efficacy of ICBs in some patients.[38] Uncovering the behind mechanisms of expression and regulation of PD-L1 in tumor microenvironment may improve the therapeutic efficacy of ICBs. p53 negatively regulates PD-L1 expression by *miR-34a* in lung cancer and cervical cancer.[19,20] Meanwhile, p53 level is frequently downregulated in CagA-positive GC.[16] In this study, CagA expression promoted PD-L1 expression in tumor tissue and increase PD-L1 level in exosomes through regulating the p53-*miR-34a*-PD-L1 signal axis, linking with the immune evasion of Hp-infected GC.

Hp CagA participates in severe gastritis, duodenal ulceration, and gastric adenocarcinoma, gastric mucosa-associated lymphoid tissue lymphoma, and gastric diffuse large B cell lymphomas.[39,40] As a grade I carcinogen of GC, the high rate of Hp infection seriously affects human health. Mechanically, through interacting with tyrosine phosphatases such as SHP2 and SHIP2 and activating oncogenic signaling pathways such as NF-κB and PI3K-AKT, CagA contributes to the development and progression of Hp-infected GC by influencing cell morphology, apoptosis, proliferation, and motility.[41–44] Exosomal PD-L1 is a key factor in regulating the prognosis and ICB therapy of GC, but the regulatory effect of CagA on tissue PD-L1 and exosomal PD-L1 is still unclear. In this study, CagA expression was found to be not only significantly associated with the elevated TNM stage but also positively correlated with the positive rate of tissue PD-L1 expression ($r = 0.332$, $p = 0.002$) and the high level of exosomal PD-L1 protein ($\rho = 0.385$, $p < 0.001$) in Hp-infected GC, highlighting the regulatory effect of CagA on supporting the malignant transformation and immune evasion of Hp-infected GC.

In summary, the current study provided evidence that exosomal PD-L1 is a prognostic factor for CagA-expressed GC that infected with Hp, and immune evasion of Hp-infected GC that contributed by the increased level of exosomal PD-L1 and the decreased anticancer effect of $CD8^+$ T cells may be regulated by the CagA-p53-*miR-34a*-PD-L1 signal axis. Targeting CagA and exosomal PD-L1 may be alternative strategies for improving the efficacy of early diagnosis and ICB therapy in Hp-infected GC.

Limitation of the study

CagA may enter into circulations via exosomes that derived from gastric epithelial cells, resulting in GC development, extragastric disorders, atherosclerosis, and intestinal epithelium barrier dysfunction.[45–47] However, the regulating effect of exosomal CagA on immune evasion of Hp-infected GC is needed in future study. Meanwhile, the Hp bacterial virulence factors such as VacA, which is similar to CagA, should be explored in follow-up study.

STAR★METHODS

Detailed methods are provided in the online version of this paper and include the following:

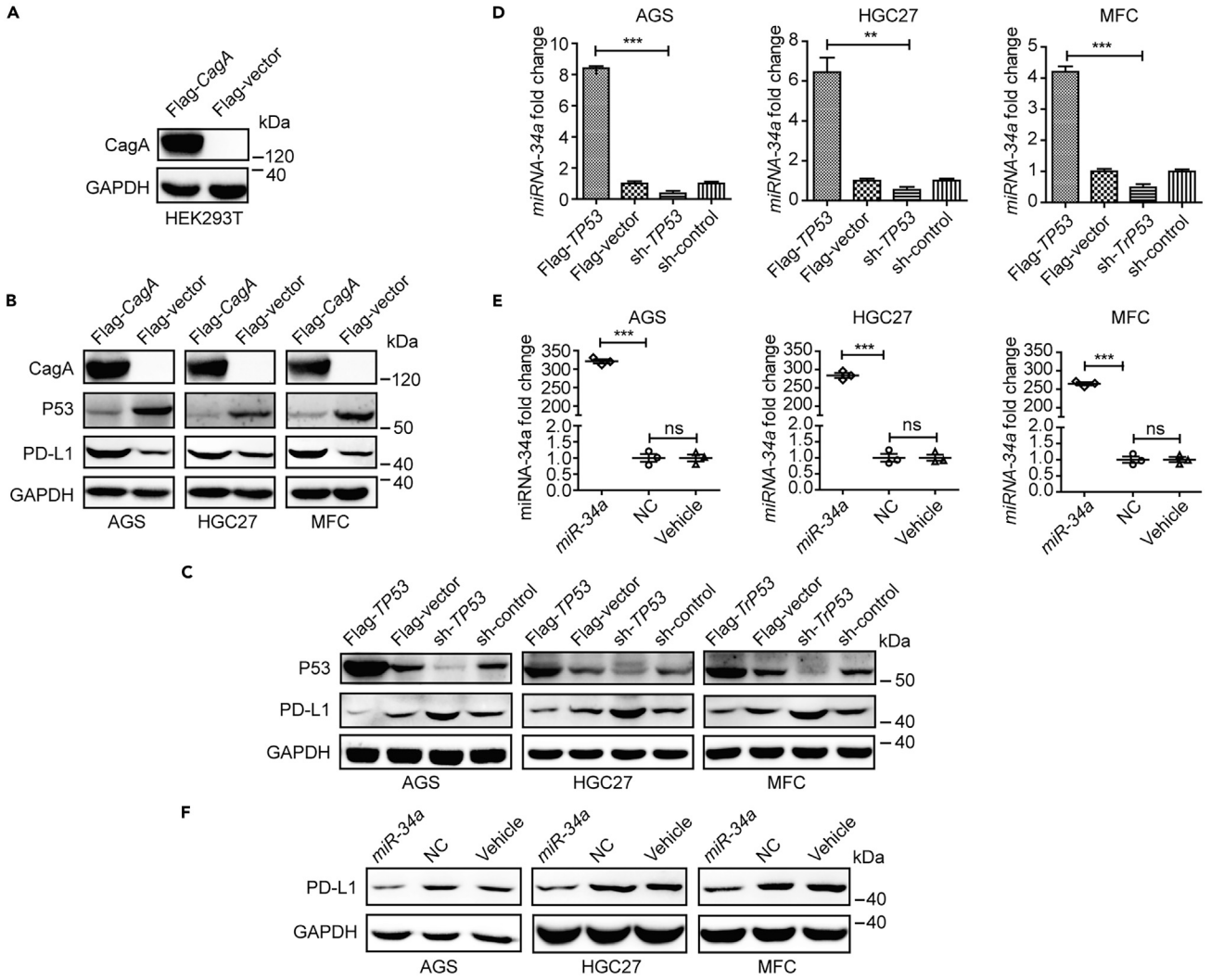

Figure 2. Regulatory effect of CagA-p53-*miR-34a* signal axis on PD-L1 expression in GC cells

(A) Western blot for Flag in HEK293T cells after transfecting Flag-vector or Flag-*CagA* plasmids for 48 h.

(B) Western blot for protein levels of Flag, P53, and PD-L1 in human GC cells AGS and HGC27 as well as mouse GC cells MFC. Cells were stably transfected with Flag-*CagA* plasmid or Flag-vector for 48 h.

(C) Western blot for protein levels of P53 and PD-L1 in human and mouse GC cells. Cells were stably transfected with Flag-*CagA* plasmid or Flag-vector for 48 h or stably infected with lentivirus sh-Control or sh-*TrP53*.

(D) qRT-PCR for *miR-34a* level in plasmid transfected and lentivirus infected GC cells of (C).

(E) qRT-PCR for *miR-34a* level in GC cells. Cells were transfected with *miR-34a* mimics or NC for 48 h.

(F) Western blot for protein level of PD-L1 in GC cells of (E). Data were analyzed by one-way ANOVA, and are represented as mean ± SD. **p < 0.01 and ***p < 0.001.

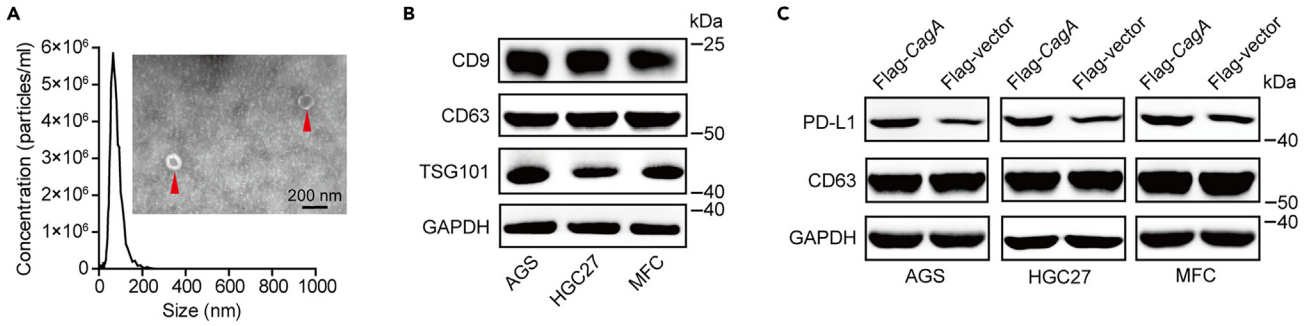

Figure 3. Influence of CagA on protein expression of exosomal PD-L1

(A) NTA and TEM for size distribution and morphology of exosomes that isolated from HGC27 cells. Scale bar, 200 nm.

(B) Western blot for protein levels of CD9, CD63, and TSG101 in AGS, HGC27, and MFC cells.

(C) Western blot for protein level of PD-L1 in exosomes derived from supernatants of cultured AGS, HGC27, and MFC cells. Cells were stably transfected with Flag-*CagA* plasmid or Flag-vector.

- METHOD DETAILS
  - Plasmid construction
  - Lentiviral package and infection

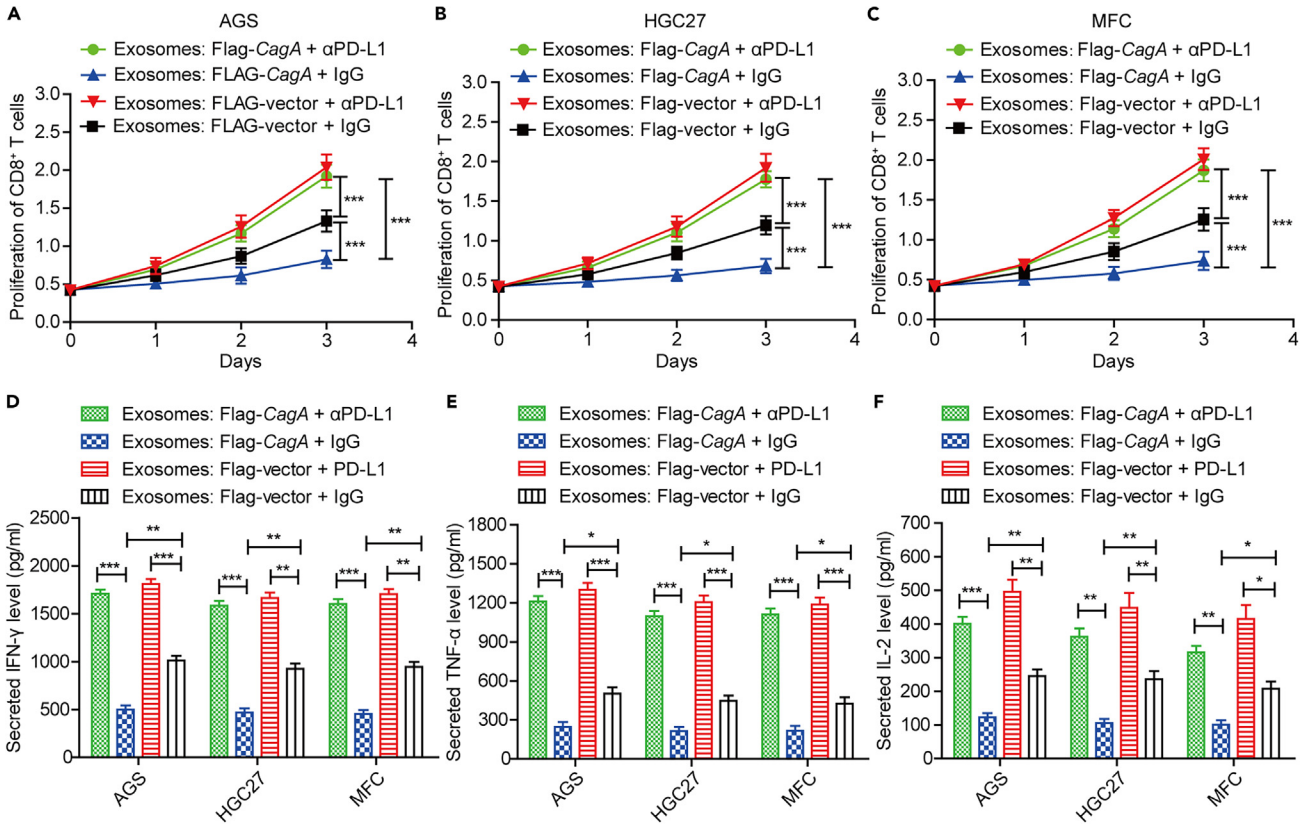

Figure 4. Influences of exosomal PD-L1 derived from GC cells including AGS, HGC27, and MFC and anti-PD-L1 antibody (αPD-L1) on CD8⁺ T cell activity

(A–C) Proliferation of $CD8^+$ T cells after treatment of exosomes with different level of PD-L1 protein derived from GC cells and treatment of αPD-L1 or IgG, as assayed by CCK8.

(D–F) Protein levels of IFN-γ (D), TNF-α (E), and IL-2 (F) that secreted by $CD8^+$ T cells after treatment of exosomes with different level of PD-L1 protein derived from GC cells and treatment of αPD-L1 or IgG, as assayed by ELISA. Data were analyzed by one-way ANOVA and are represented as mean ± SD. *$p < 0.05$, **$p < 0.01$, and ***$p < 0.001$.

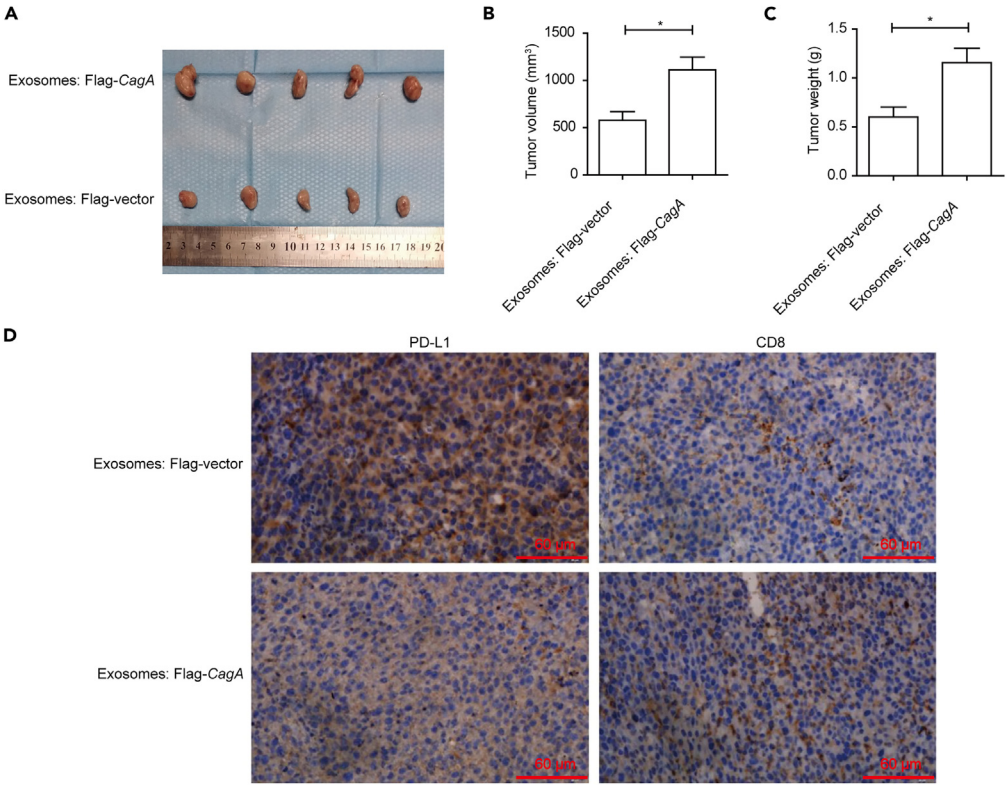

Figure 5. Influence of exosomes with high level of PD-L1 derived from *CagA*-transfected GC Cells on tumor growth and immune evasion

(A) Image of formed tumor in mice. 5 × 10^6 MFC cells were administered to the 615 mice by subcutaneous injection. After the formation of visible tumors, exosomes derived from Flag-*CagA* plasmid or Flag-vector transfected MFC cells were administered into mice by tail vein injection.

(B and C) Statistical analyses for the volume and weight of formed tumor in (A).

(D) IHC staining for protein levels of PD-L1 and CD8 in formed tumors in (A). Scale bar, 60 μm. Data were analyzed by two-sided Student's t tests and are represented as mean ± SD. *p < 0.05.

ACKNOWLEDGMENTS

We would like to thank Dr. Hailong Xie (Nanhua University) for providing genomic DNA derived from $CagA^+$ Hp strain 26695, and Dr. Luolin Wang (Hunan University) for providing cDNA derived from RAW264.7 cells. This study was supported by the National Natural Science Foundation of China (82170192 to C.Z.), and the China Postdoctoral Science Foundation (2021M701151 to R.D.).

AUTHOR CONTRIBUTIONS

J.W., R.D., and C.Z. conceived and designed the study. J.W., R.D., S.D., Q.H., B.X., Z.H., M.P., and S.L. conducted most experiments and analyzed data. J.W., Q.H., and B.X. conducted animal experiments. J.W., R.D., and J.L. performed IHC staining. Z.H., T.M., Z.C., H.Z., and C.Z. supervised the study. J.W. wrote the original paper. R.D. and C.Z. revised the manuscript. C.Z. and R.D. contributed to funding acquisition. All authors have read and agreed to the final manuscript.

DECLARATION OF INTERESTS

The authors declare no competing interests.

INCLUSION AND DIVERSITY

We support inclusive, diverse, and equitable conduct of research.

Received: July 3, 2023
Revised: October 1, 2023
Accepted: November 2, 2023
Published: November 9, 2023

REFERENCES

1. Thrift, A.P., and El-Serag, H.B. (2020). Burden of Gastric Cancer. Clin. Gastroenterol. Hepatol. *18*, 534–542.
2. Li, K., Zhang, A., Li, X., Zhang, H., and Zhao, L. (2021). Advances in clinical immunotherapy for gastric cancer. Biochim. Biophys. Acta. Rev. Cancer *1876*, 188615.
3. Wroblewski, L.E., Peek, R.M., Jr., and Wilson, K.T. (2010). Helicobacter pylori and gastric cancer: factors that modulate disease risk. Clin. Microbiol. Rev. *23*, 713–739.
4. Xue, C., Chu, Q., Zheng, Q., Yuan, X., Su, Y., Bao, Z., Lu, J., and Li, L. (2023). Current understanding of the intratumoral microbiome in various tumors. Cell Rep. Med. *4*, 100884.
5. Park, C.H., Hong, C., Lee, A.R., Sung, J., and Hwang, T.H. (2022). Multi-omics reveals microbiome, host gene expression, and immune landscape in gastric carcinogenesis. iScience *25*, 103956.
6. Kono, K., Nakajima, S., and Mimura, K. (2020). Current status of immune checkpoint inhibitors for gastric cancer. Gastric Cancer *23*, 565–578.
7. Lerrer, S., Tocheva, A.S., Bukhari, S., Adam, K., and Mor, A. (2021). PD-1-stimulated T cell subsets are transcriptionally and functionally distinct. iScience *24*, 103020.
8. Figueroa-Protti, L., Soto-Molinari, R., Calderón-Osorno, M., Mora, J., and Alpízar-Alpízar, W. (2019). Gastric Cancer in the Era of Immune Checkpoint Blockade. J. Oncol. *2019*, 1079710.
9. Li, X., Pan, K., Vieth, M., Gerhard, M., Li, W., and Mejías-Luque, R. (2022). JAK-STAT1 Signaling Pathway Is an Early Response to Helicobacter pylori Infection and Contributes to Immune Escape and Gastric Carcinogenesis. Int. J. Mol. Sci. *23*, 4147.
10. Shen, B., Qian, A., Lao, W., Li, W., Chen, X., Zhang, B., Wang, H., Yuan, F., and Sun, Y. (2019). Relationship between Helicobacter pylori and expression of programmed death-1 and its ligand in gastric intraepithelial neoplasia and early-stage gastric cancer. Cancer Manag. Res. *11*, 3909–3919.
11. Beswick, E.J., Pinchuk, I.V., Das, S., Powell, D.W., and Reyes, V.E. (2007). Expression of the programmed death ligand 1, B7-H1, on gastric epithelial cells after Helicobacter pylori exposure promotes development of CD4+ CD25+ FoxP3+ regulatory T cells. Infect. Immun. *75*, 4334–4341.
12. Das, S., Suarez, G., Beswick, E.J., Sierra, J.C., Graham, D.Y., and Reyes, V.E. (2006). Expression of B7-H1 on gastric epithelial cells: its potential role in regulating T cells during Helicobacter pylori infection. J. Immunol. *176*, 3000–3009.
13. Deng, R., Zheng, H., Cai, H., Li, M., Shi, Y., and Ding, S. (2022). Effects of helicobacter pylori on tumor microenvironment and immunotherapy responses. Front. Immunol. *13*, 923477.
14. Reyes, V.E. (2023). Helicobacter pylori and Its Role in Gastric Cancer. Microorganisms *11*, 1312.
15. Hatakeyama, M. (2014). Helicobacter pylori CagA and gastric cancer: a paradigm for hit-and-run carcinogenesis. Cell Host Microbe *15*, 306–316.
16. Yong, X., Tang, B., Li, B.S., Xie, R., Hu, C.J., Luo, G., Qin, Y., Dong, H., and Yang, S.M. (2015). Helicobacter pylori virulence factor CagA promotes tumorigenesis of gastric cancer via multiple signaling pathways. Cell Commun. Signal. *13*, 30.
17. Wei, J., Nagy, T.A., Vilgelm, A., Zaika, E., Ogden, S.R., Romero-Gallo, J., Piazuelo, M.B., Correa, P., Washington, M.K., El-Rifai, W., et al. (2010). Regulation of p53 tumor suppressor by Helicobacter pylori in gastric epithelial cells. Gastroenterology *139*, 1333–1343.
18. Buti, L., Spooner, E., Van der Veen, A.G., Rappuoli, R., Covacci, A., and Ploegh, H.L. (2011). Helicobacter pylori cytotoxin-associated gene A (CagA) subverts the apoptosis-stimulating protein of p53 (ASPP2) tumor suppressor pathway of the host. Proc. Natl. Acad. Sci. USA *108*, 9238–9243.
19. Cortez, M.A., Ivan, C., Valdecanas, D., Wang, X., Peltier, H.J., Ye, Y., Araujo, L., Carbone, D.P., Shilo, K., Giri, D.K., et al. (2016). PDL1 Regulation by p53 via miR-34. J. Natl. Cancer Inst. *108*, djv303.
20. Xu, S., Wang, X., Yang, Y., Li, Y., and Wu, S. (2021). LSD1 silencing contributes to enhanced efficacy of anti-CD47/PD-L1 immunotherapy in cervical cancer. Cell Death Dis. *12*, 282.
21. Wang, X., Li, J., Dong, K., Lin, F., Long, M., Ouyang, Y., Wei, J., Chen, X., Weng, Y., He, T., and Zhang, H. (2015). Tumor suppressor miR-34a targets PD-L1 and functions as a potential immunotherapeutic target in acute myeloid leukemia. Cell. Signal. *27*, 443–452.
22. Huang, X., Xie, X., Wang, H., Xiao, X., Yang, L., Tian, Z., Guo, X., Zhang, L., Tang, H., and Xie, X. (2017). PDL1 And LDHA act as ceRNAs in triple negative breast cancer by regulating miR-34a. J. Exp. Clin. Cancer Res. *36*, 129.
23. Anastasiadou, E., Stroopinsky, D., Alimperti, S., Jiao, A.L., Pyzer, A.R., Cippitelli, C., Pepe, G., Severa, M., Rosenblatt, J., Etna, M.P., et al. (2019). Epstein-Barr virus-encoded EBNA2 alters immune checkpoint PD-L1 expression by downregulating miR-34a in B-cell lymphomas. Leukemia *33*, 132–147.
24. Gurung, S., Perocheau, D., Touramanidou, L., and Baruteau, J. (2021). The exosome journey: from biogenesis to uptake and intracellular signalling. Cell Commun. Signal. *19*, 47.
25. Kimiz-Gebologlu, I., and Oncel, S.S. (2022). Exosomes: Large-scale production, isolation, drug loading efficiency, and biodistribution and uptake. J. Control Release. *347*, 533–543.
26. Huang, T., and Deng, C.X. (2019). Current Progresses of Exosomes as Cancer Diagnostic and Prognostic Biomarkers. Int. J. Biol. Sci. *15*, 1–11.
27. Fan, Y., Che, X., Qu, J., Hou, K., Wen, T., Li, Z., Li, C., Wang, S., Xu, L., Liu, Y., and Qu, X. (2019). Exosomal PD-L1 Retains Immunosuppressive Activity and is Associated with Gastric Cancer Prognosis. Ann. Surg Oncol. *26*, 3745–3755.
28. Poggio, M., Hu, T., Pai, C.C., Chu, B., Belair, C.D., Chang, A., Montabana, E., Lang, U.E., Fu, Q., Fong, L., and Blelloch, R. (2019). Suppression of Exosomal PD-L1 Induces Systemic Anti-tumor Immunity and Memory. Cell *177*, 414–427.e13.
29. Zhang, M., Dong, Y., Liu, H., Wang, Y., Zhao, S., Xuan, Q., Wang, Y., and Zhang, Q. (2016). The clinicopathological and prognostic significance of PD-L1 expression in gastric cancer: a meta-analysis of 10 studies with 1,901 patients. Sci. Rep. *6*, 37933.
30. Xing, X., Guo, J., Ding, G., Li, B., Dong, B., Feng, Q., Li, S., Zhang, J., Ying, X., Cheng, X., et al. (2018). Analysis of PD1, PDL1, PDL2 expression and T cells infiltration in 1014 gastric cancer patients. OncoImmunology *7*, e1356144.
31. Paskeh, M.D.A., Entezari, M., Mirzaei, S., Zabolian, A., Saleki, H., Naghdi, M.J., Sabet, S., Khoshbakht, M.A., Hashemi, M., Hushmandi, K., et al. (2022). Emerging role of exosomes in cancer progression and tumor microenvironment remodeling. J. Hematol. Oncol. *15*, 83.
32. LeBleu, V.S., and Kalluri, R. (2020). Exosomes as a Multicomponent Biomarker Platform in Cancer. Trends Cancer *6*, 767–774.
33. He, J., Tsai, L.M., Leong, Y.A., Hu, X., Ma, C.S., Chevalier, N., Sun, X., Vandenberg, K., Rockman, S., Ding, Y., et al. (2013). Circulating precursor CCR7(lo)PD-1(hi) CXCR5(+) CD4(+) T cells indicate Tfh cell activity and promote antibody responses upon antigen reexposure. Immunity *39*, 770–781.
34. Ahn, E., Araki, K., Hashimoto, M., Li, W., Riley, J.L., Cheung, J., Sharpe, A.H., Freeman, G.J., Irving, B.A., and Ahmed, R. (2018). Role of PD-1 during effector CD8 T cell differentiation. Proc. Natl. Acad. Sci. USA *115*, 4749–4754.

35. Chen, D., Tan, S., Zhang, H., Wang, H., He, W., Shi, R., Tong, Z., Zhu, J., Cheng, H., Gao, S., et al. (2019). The FG Loop of PD-1 Serves as a "Hotspot" for Therapeutic Monoclonal Antibodies in Tumor Immune Checkpoint Therapy. iScience *14*, 113–124.
36. Zhao, L., Zhang, W., Luan, F., Chen, X., Wu, H., He, Q., Weng, Q., Ding, L., and Yang, B. (2023). Butein suppresses PD-L1 expression via downregulating STAT1 in non-small cell lung cancer. Biomed. Pharmacother. *157*, 114030.
37. Kim, D.H., Kim, H., Choi, Y.J., Kim, S.Y., Lee, J.E., Sung, K.J., Sung, Y.H., Pack, C.G., Jung, M.K., Han, B., et al. (2019). Exosomal PD-L1 promotes tumor growth through immune escape in non-small cell lung cancer. Exp. Mol. Med. *51*, 1–13.
38. Chen, G., Huang, A.C., Zhang, W., Zhang, G., Wu, M., Xu, W., Yu, Z., Yang, J., Wang, B., Sun, H., et al. (2018). Exosomal PD-L1 contributes to immunosuppression and is associated with anti-PD-1 response. Nature *560*, 382–386.
39. Kuo, S.H., Chen, L.T., Lin, C.W., Yeh, K.H., Shun, C.T., Tzeng, Y.S., Liou, J.M., Wu, M.S., Hsu, P.N., and Cheng, A.L. (2017). Expressions of the CagA protein and CagA-signaling molecules predict Helicobacter pylori dependence of early-stage gastric DLBCL. Blood *129*, 188–198.
40. Eck, M., Schmausser, B., Haas, R., Greiner, A., Czub, S., and Müller-Hermelink, H.K. (1997). MALT-type lymphoma of the stomach is associated with Helicobacter pylori strains expressing the CagA protein. Gastroenterology *112*, 1482–1486.
41. Higashi, H., Tsutsumi, R., Muto, S., Sugiyama, T., Azuma, T., Asaka, M., and Hatakeyama, M. (2002). SHP-2 tyrosine phosphatase as an intracellular target of Helicobacter pylori CagA protein. Science *295*, 683–686.
42. Fujii, Y., Murata-Kamiya, N., and Hatakeyama, M. (2020). Helicobacter pylori CagA oncoprotein interacts with SHIP2 to increase its delivery into gastric epithelial cells. Cancer Sci. *111*, 1596–1606.
43. Yoon, J.H., Seo, H.S., Choi, S.S., Chae, H.S., Choi, W.S., Kim, O., Ashktorab, H., Smoot, D.T., Nam, S.W., Lee, J.Y., and Park, W.S. (2014). Gastrokine 1 inhibits the carcinogenic potentials of Helicobacter pylori CagA. Carcinogenesis *35*, 2619–2629.
44. Higashi, H., Nakaya, A., Tsutsumi, R., Yokoyama, K., Fujii, Y., Ishikawa, S., Higuchi, M., Takahashi, A., Kurashima, Y., Teishikata, Y., et al. (2004). Helicobacter pylori CagA induces Ras-independent morphogenetic response through SHP-2 recruitment and activation. J. Biol. Chem. *279*, 17205–17216.
45. Lin, T.Y., Lan, W.H., Chiu, Y.F., Feng, C.L., Chiu, C.H., Kuo, C.J., and Lai, C.H. (2021). Statins' Regulation of the Virulence Factors of Helicobacter pylori and the Production of ROS May Inhibit the Development of Gastric Cancer. Antioxidants *10*, 1293.
46. Shimoda, A., Ueda, K., Nishiumi, S., Murata-Kamiya, N., Mukai, S.A., Sawada, S.i., Azuma, T., Hatakeyama, M., and Akiyoshi, K. (2016). Exosomes as nanocarriers for systemic delivery of the Helicobacter pylori virulence factor CagA. Sci. Rep. *6*, 18346.
47. Yang, S., Xia, Y.P., Luo, X.Y., Chen, S.L., Li, B.W., Ye, Z.M., Chen, S.C., Mao, L., Jin, H.J., Li, Y.N., and Hu, B. (2019). Exosomal CagA derived from Helicobacter pylori-infected gastric epithelial cells induces macrophage foam cell formation and promotes atherosclerosis. J. Mol. Cell. Cardiol. *135*, 40–51.
48. Deng, R., Zuo, C., Li, Y., Xue, B., Xun, Z., Guo, Y., Wang, X., Xu, Y., Tian, R., Chen, S., et al. (2020). The innate immune effector ISG12a promotes cancer immunity by suppressing the canonical Wnt/β-catenin signaling pathway. Cell. Mol. Immunol. *17*, 1163–1179.
49. Carter, B.Z., Mak, D.H., Schober, W.D., Dietrich, M.F., Pinilla, C., Vassilev, L.T., Reed, J.C., and Andreeff, M. (2008). Triptolide sensitizes AML cells to TRAIL-induced apoptosis via decrease of XIAP and p53-mediated increase of DR5. Blood *111*, 3742–3750.
50. Dickins, R.A., McJunkin, K., Hernando, E., Premsrirut, P.K., Krizhanovsky, V., Burgess, D.J., Kim, S.Y., Cordon-Cardo, C., Zender, L., Hannon, G.J., and Lowe, S.W. (2007). Tissue-specific and reversible RNA interference in transgenic mice. Nat. Genet. *39*, 914–921.
51. Kuo, S.H., Chen, L.T., Lin, C.W., Wu, M.S., Hsu, P.N., Tsai, H.J., Chu, C.Y., Tzeng, Y.S., Wang, H.P., Yeh, K.H., and Cheng, A.L. (2013). Detection of the Helicobacter pylori CagA protein in gastric mucosa-associated lymphoid tissue lymphoma cells: clinical and biological significance. Blood Cancer J. *3*, e125.
52. Eto, S., Yoshikawa, K., Nishi, M., Higashijima, J., Tokunaga, T., Nakao, T., Kashihara, H., Takasu, C., Iwata, T., and Shimada, M. (2016). Programmed cell death protein 1 expression is an independent prognostic factor in gastric cancer after curative resection. Gastric Cancer *19*, 466–471.
53. Zhang, P.F., Gao, C., Huang, X.Y., Lu, J.C., Guo, X.J., Shi, G.M., Cai, J.B., and Ke, A.W. (2020). Cancer cell-derived exosomal circUHRF1 induces natural killer cell exhaustion and may cause resistance to anti-PD1 therapy in hepatocellular carcinoma. Mol. Cancer *19*, 110.

STAR★METHODS

KEY RESOURCES TABLE

REAGENT or RESOURCE	SOURCE	IDENTIFIER
Antibodies		
Mouse anti-CagA	Santa Cruz Biotechnology	Cat# sc-28368; RRID: AB_628229
Mouse anti-p53	Abcam	Cat# ab26; RRID: AB_303198
Rabbit anti-PD-L1	Proteintech	Cat# 17952-1-AP; RRID: AB_10597552
Rabbit anti-CD63	System Biosciences	Cat# EXOAB-CD63A-1; RRID: AB_2561274
Rabbit anti-CD9	Cell Signaling Technology	Cat# 13174S; RRID: AB_2798139
Rabbit anti-TSG101	System Biosciences	Cat# EXOAB-TSG101-1
Mouse anti-GAPDH	Merck Millipore	Cat# MAB374; RRID: AB_2107445
Rabbit anti-CD8	Abcam	Cat# ab4055; RRID: AB_304247
Goat anti-mouse IgG (HRP-linked)	Merck Millipore	Cat# AP124P; RRID: AB_90456
Goat anti-rabbit IgG (HRP-linked)	Merck Millipore	Cat# AP132P; RRID: AB_90264
InVivoMAb anti-human PD-L1 (B7-H1)	Bio X Cell	Cat# BE0285; RRID:AB_2687808
InVivoPlus anti-mouse PD-L1 (B7-H1)	Bio X Cell	Cat# BE0101; RRID: AB_10949073
InVivoPlus mouse IgG2b isotype control	Bio X Cell	Cat# BE0086; RRID: AB_1107791
Rat IgG2b I sotype control	Bio X Cell	Cat# BE0090; RRID: AB_1107780
GMP Ultra-LEAF™ Purified anti-human CD3 SF	BioLegend	Cat# 317353; RRID: AB_2894461
Ultra-LEAF™ Purified anti-mouse CD3ε Antibody	BioLegend	Cat# 100339; RRID: AB_11150783
Ultra-LEAF™ Purified anti-human CD28 (Superagonistic) Antibody	BioLegend	Cat# 377803; RRID: AB_2910434
Ultra-LEAF™ Purified anti-mouse CD28 Antibody	BioLegend	Cat# 102115; RRID: AB_11150408
Bacterial and virus strains		
E. coli DH5α competent cells	Lab stock	N/A
E. coli. Stable competent cells	Lab stock	N/A
Hp strain 26695	Hailong Xie, Nanhua University	N/A
Lentivirus-expressing sh-control	This paper	N/A
Lentivirus-expressing sh-*TP53*	This paper	N/A
Lentivirus-expressing sh-*TrP53*	This paper	N/A
Biological samples		
Peripheral blood of GC patients	Hunan Cancer Hospital	N/A
Peripheral blood of healthy individuals	Hunan Cancer Hospital	N/A
Human GC tissue specimens	Hunan Cancer Hospital	N/A
Mouse tissue specimens	Hunan Cancer Hospital	N/A
Spleens of 615 mouse	Junke biological	N/A
Chemicals, peptides, and recombinant proteins		
Puromycin	Thermo Fisher Scientific	Cat# A1113803
TRIzol reagent	Thermo Fisher Scientific	Cat# 15596018
Proteinase inhibitor cocktail	Thermo Fisher Scientific	Cat# 7843
RIPA buffer	Thermo Fisher Scientific	Cat# 89900
Lympholyte®-H (human)	Cedarlane	Cat# CL5015-R
Lympholyte®-M (mouse)	Cedarlane	Cat# CL5031
Collagenase II	Thermo Fisher Scientific	Cat# 17101015

(*Continued on next page*)

Continued

REAGENT or RESOURCE	SOURCE	IDENTIFIER
Blue Plus® II Western Marker	Transgen Biotech	Cat# DM111-02
CCK8	Dojindo	Cat# CK04
DAB	BOSTER	Cat# AR1022
Hematoxylin	BOSTER	Cat# AR0005
Critical commercial assays		
KOD-Plus-Neo	TOYOBO	Cat# KOD-401
QIAprep Spin Miniprep Kit	QIAGEN	Cat# 27104
All-in-OneTM miRNA qRT-PCR Detection kit	GeneCopoeia	Cat# QP115
SuperSignal® West Pico Chemiluminescent Substrate	Thermo Fisher Scientific	Cat# 34578
ExoQuick Plasma Prep with Thrombin	System Biosciences	Cat# EXOQ5TM-1
MojoSort™ Human CD8 Naive T cell Isolation Kit	BioLegend	Cat# 480045
MojoSort™ Mouse CD8 Naive T cell Isolation Kit	BioLegend	Cat# 480043
IFN gamma ELISA Kit, Human	Sino Biological	Cat# SEK13222
IFNAR1 Matched ELISA Antibody Pair Set, Mouse	Sino Biological	Cat# SEK50469
TNF-alpha ELISA Kit, Human	Sino Biological	Cat# KIT10602
TNF-alpha Matched ELISA Antibody Pair Set, Mouse	Sino Biological	Cat# SEK50349
IL2 ELISA Kit, Human	Sino Biological	Cat# KIT11848
IL2RG Matched ELISA Antibody Pair Set,Mouse	Sino Biological	Cat# SEK50087
Experimental models: Cell lines		
HGC-27	Stem Cell Bank, Chinese Academy of Sciences	RRID: CVCL_1279
AGS	Kunming cell bank of the typical culture preservation Committee of the Chinese Academy of Sciences	RRID: CVCL_0139
MFC	Kunming cell bank of the typical culture preservation Committee of the Chinese Academy of Sciences	RRID: CVCL_5J48
HEK293T	ATCC	RRID: CVCL_0063
Human $CD8^+$ T cell	Peripheral blood	N/A
Mouse $CD8^+$ T cell	Spleens of 615 mouse	N/A
Experimental models: Organisms/strains		
615 mouse	Junke biological Co., LTD.	RRID: MGI:2669495
Oligonucleotides		
shRNA targeting sequence: sh-control: ACTACCGTTGTTATAGGTG	Deng et al. Cell. Mol. Immunol. 17, 1163-1179[48]	N/A
shRNA targeting sequence: sh-*TP53*: GACTCCAGTGGTAATCTAC	Carter et al. Blood 111, 3742-3750[49]	N/A
shRNA targeting sequence: sh-*TrP53*: CACTACAAGTACATGTGTA	Dickins et al. Nat. Genet. 39, 914-921[50]	N/A
Primers: p3×Flag-*CagA* forward: GCTCT AGAGCCACCATGACTAACGAAACTATTGAT	This paper	N/A
Primers: p3×Flag-*CagA* reverse: CGGG ATCCAGATTTTTGGAAACCACCTTTTGT	This paper	N/A
Primers: p3×Flag-*TP53* forward: GGAATTCC ACCATGGAGGAGCCGCAGTCAG	This paper	N/A

(*Continued on next page*)

Continued

REAGENT or RESOURCE	SOURCE	IDENTIFIER
Primers: p3×Flag-*TP53* reverse: TGCTCTA GAGTCTGAGTCAGGCCCTTCTGTC	This paper	N/A
Primers: p3×Flag-*TrP53* forward: GGAATTCC ACCATGACTGCCATGGAGGAGTCACAG	This paper	N/A
Primers: p3×Flag-*TrP53* reverse: GCTCTA GAGTCTGAGTCAGGCCCCACTTTC	This paper	N/A
Recombinant DNA		
p3×Flag-*CagA*	This paper	N/A
p3xFlag-CMV-14	This paper	N/A
p3×Flag-*TP53* (human)	This paper	N/A
p3×Flag-*TrP53* (mouse)	This paper	N/A
pGreenPuro shRNA Lentivector	System Biosciences	Cat# SI505A-1
sh-control	This paper	N/A
sh-*TP53* (human)	This paper	N/A
sh-*TrP53* (mouse)	This paper	N/A
psPAX2	Addgene	Cat# 12260; RRID: Addgene_12260
pMD2.G	Addgene	Cat# 12259; RRID: Addgene_12259
Software and algorithms		
SPSS 22.0 software	IBM Corporation	https://www.ibm.com/support/pages/spss-statistics-220-available-download
GraphPad Prism 8.0 software	GraphPad	https://www.graphpad.com/
ImageJ software	ImageJ	https://ImageJ.en.softonic.com/mac
Other		
DMEM	Thermo Fisher Scientific	Cat# C11965500BT
FBS	Thermo Fisher Scientific	Cat# 10270-106
Penicillin-Streptomycin	Thermo Fisher Scientific	Cat# 15140122
RPMI1640 medium	Thermo Fisher Scientific	Cat# C11875500BT
Opti-MEM™ serum-free medium	Thermo Fisher Scientific	Cat# 31985088
Lipofectamine® 2000	Thermo Fisher Scientific	Cat# 11668019

RESOURCE AVAILABILITY

Lead contact

Further information and requests for resources and reagents should be directed to and will be fulfilled by the lead contact, Chaohui Zuo (zuochaohui@vip.sina.com).

Materials availability

This study did not generate new unique reagents. All the cell lines used in this manuscript will be made available upon request. A material transfer agreement will be required prior to sharing of materials.

Data and code availability

- Date: Data reported in this paper will be shared by the lead contact upon request.
- Code: This paper does not report original code.
- All other requests: Any additional information required to reanalyze the data reported will be shared by the lead contact upon request.

EXPERIMENTAL MODEL AND STUDY PARTICIPANT DETAILS

Ethics approval and consent to participate

Studies involved in human participants were approved by Ethics Committee of Hunan Cancer Hospital (No. KYJJ-2021-073) and conducted in compliance with the tenets of the Declaration of Helsinki. All patients provided written informed consent under approval by the Ethics Committee of Hunan Cancer Hospital. Protocol used for animal experiments was approved by the Animal Care and Experiment Committee of Hunan Cancer Hospital (No. GZ2023-049). All the authors consented to participate in this study.

Clinical samples

From January 2019 to December 2020, a total of 87 patients that pathologically diagnosed with GC at Hunan Cancer Hospital were recruited for this study. Plasmas from preoperative peripheral blood of 87 GC patients used for extracting exosomes were preserved in a −20°C refrigerator, and 87 tumor specimens used for IHC staining were fixed with formalin and embedded into paraffin. Clinical samples were divided into groups according to the median value of PD-L1 protein level in plasma exosomes and the positive expression of CagA, P53, and PD-L1 proteins in tumor tissues. The diagnosis of GC was established according to the histopathological and immunohistochemical criteria in 2016 WHO classification system. The inclusion and exclusion criterion are as follows: (1) postoperative pathological diagnosis was gastric adenocarcinoma; (2) preoperative gastroscopy confirmed HP infection; (3) peripheral blood samples were retained before operation; (4) received surgical treatment without cancer history and anticancer treatment before operation; (5) had complete pathological, clinical, and follow-up data; (6) patients or their families agreed that their postoperative pathological specimens, preoperative peripheral blood specimens, and medical records should be used for scientific research. All patients were traced every 3–6 months by outpatient or telephone follow-up, and the last follow-up date was in December 2021. Clinical samples were collected with the approval of the Ethics Committee of Hunan Cancer Hospital.

Cell lines

Human GC cell line HGC27 (RRID: CVCL_3360) was obtained from the Stem Cell Bank, Chinese Academy of Sciences (Shanghai, China), human GC cell line AGS (RRID: CVCL_0139) and mouse GC cell line MFC (RRID: CVCL_5J48) were obtained from the Kunming cell bank of the typical culture preservation Committee of the Chinese Academy of Sciences (Kunming, China). Human embryonic kidney fibroblast cell line HEK293T (RRID: CVCL_0063) was purchased from ATCC (Manassas, USA). Human $CD8^+$ T cells were isolated from peripheral blood of healthy individuals, and mouse $CD8^+$ T cells were isolated from spleens of 615 mice. HGC27 cells and HEK293T cells were cultivated in DMEM (Thermo Fisher Scientific, USA) supplemented with 10% (v/v) FBS (Thermo Fisher Scientific), and AGS cells and MFC cells were cultivated in RPMI 1640 medium (Thermo Fisher Scientific) supplemented with 10% (v/v) FBS (Thermo Fisher Scientific). Cells were cultured in an incubator with 95% humidity and 5% CO_2 at 37°C, which were authenticated by STR profiling at the time of receipt and periodically thereafter.

Mice

The five-week-old male 615 mice (Junke biological, Nanjing, China) were fed under standard conditions (temperature, 25°C; humidity, 40–60%; 12-h light/dark cycle; free access to standard sterile food and water) in a pathogen-free environment at the animal care facility of Hunan University. Protocol used for animal experiments was approved by the Animal Care and Experiment Committee of Hunan Cancer Hospital.

METHOD DETAILS

Plasmid construction

Genomic DNA extracted from Hp strain 26695 was used for constructing plasmids with *CagA* expression. The cDNA used for constructing expression plasmid of *TP53* (human) was synthesized using total cellular RNA isolated from HEK293T cells, and the cDNA synthesized using total RNA derived from RAW264.7 cells applied for constructing expression plasmid of *TrP53* (mouse). The sequences used for plasmid construction were obtained with the high-fidelity PCR kit KOD-Plus-Neo (TOYOBO, Japan), which were further cloned into the p3×Flag-CMV-14 vector (Sigma-Aldrich, Germany) according to our previous research.[48] Plasmids constructed using p3×Flag-vector express the FLAG tag. The specific primers used for plasmid construction are listed in key resources table. The short hairpin RNAs (shRNAs) targeting *TP53* (human) or *TrP53* (mouse) was constructed using the pGreenPuro shRNA Lentivector (System Biosciences, USA) according to the manufacturer's instructions. The target sequences of shRNAs for silencing *TP53* (human) (sh-*TP53*),[49] *TrP53* (mouse) (sh-*TrP53*),[50] and the negative control (sh-control)[48] are listed in key resources table. Plasmids were amplified in *E. coli* DH5α and *Stable* competent cells, sequenced at Sangon Biotech (Shanghai, China), and isolated using QIAprep Spin Miniprep Kit (Qiagen, Germany).

Lentiviral package and infection

HEK293T cells were seeded into 100 mm dishes at a cell coverage between 60% and 70%. After cultivation for 24 h, 8.0 μg of gene silencing, 8.0 μg of lentiviral packaging plasmid psPAX2, and 2.7 μg of envelope plasmid pMD2G were mixed into 300 μL of Opti-MEM serum-free medium, and 18 μL of Lipofectamine 2000 was mixed into 300 μL of Opti-MEM serum-free medium for 5 min, which were mixed together and incubated at room temperature for 20 min. Then, the incubated mixtures were added into the culture medium of HEK293T cells. After cell

transfection for 48 h, supernatants containing virus particles was collected and filtered using 0.45 μm filters, which were added into culture medium of cells with approximately 30–40% coverage. Puromycin (Thermo Fisher Scientific) was added to culture medium to screen the stably infected cells after cell infection with lentivirus for 72 h.

Cell transfection

Cell transfection of plasmids and *miR-34a* oligonucleotides was conducted using Lipofectamine 2000 (Thermo Fisher Scientific) in Opti-MEM medium (Thermo Fisher Scientific) according to the manufacturer's instruction. In brief, cells in the logarithmic phase were seeded in 6-well plates (Corning Incorporated) at about 60% confluence. After cultivation for 24 h, cells in per well of 6-well plates were transfected with 2 ng of plasmids or 25 nmol of *miR-34a* oligonucleotides in 200 μL of Opti-MEM medium supplemented with 6 μL of Lipofectamine 2000 (Thermo Fisher Scientific). After cell transfection for 48 h–72 h, the expression levels of target RNAs and proteins were examined by qRT-PCR or Western blot. The stably transfected cells were screened using 8 μg/mL puromycin (Sigma-Aldrich) for 15 days.

Quantitative real-time PCR (qRT-PCR)

qRT-PCR was performed using All-in-One miRNA qRT-PCR Detection kit (GeneCopoeia, USA) on ABI PRISM 7700 instrument (PerkinElmer Applied Biosystems, USA). Total RNA was extracted from cells using TRIzol reagent (Thermo Fisher Scientific). The specific primers of *miR-34a* (5′-TGGCAGTGTCTTAGCTGGTTG-3′) and internal control *U6* were commercially obtained (GeneCopoeia, USA). The relative level of *miR-34a* was calculated by the $2^{-\Delta\Delta Ct}$ method.

Western blot

Cells were lysed with RIPA buffer (Thermo Fisher Scientific) supplemented with a proteinase inhibitor cocktail (Thermo Fisher Scientific). After incubation on ice for 30 min, the lysates were centrifuged at 16 100 × g and 4°C for 15 min, and the protein-containing supernatants were collected for examination. After determining the protein concentration by BCA method, total protein was electrophoresed along with the Blue Plus II Western Marker (Transgen Biotech, China) on SDS-PAGE gels and transferred onto PVDF membranes (Merck Millipore, Germany). The PVDF membranes were then blocked with 5% skim milk, sequentially incubated with primary antibodies at 4°C overnight and secondary antibodies at room temperature for 2 h, and detected using SuperSignal West Pico Chemiluminescent Substrate (Thermo Fisher Scientific). Following antibodies were commercially obtained and used for Western blot: mouse anti-CagA (clone A-10, sc-28368, Santa Cruz, USA), mouse anti-p53 (clone PAb 240, ab26, Abcam, UK), rabbit anti-PD-L1 (17952-1-AP, Proteintech, USA), rabbit anti-CD63 (EXOAB-CD63A-1, System Biosciences), rabbit anti-CD9 (clone D8O1A, 13174S, CST, USA), rabbit anti-TSG101(EXOAB-TSG101-1, System Biosciences), mouse anti-GAPDH (clone 6C5, MAB374, Merck Millipore, USA), goat anti-mouse IgG (HRP-linked) (AP124P, Merck Millipore), and goat anti-rabbit IgG (HRP-linked) (AP132P, Merck Millipore). The investigators were blinded to the identity of the tissue specimens during experiments.

IHC staining

Tissue samples were obtained immediately after surgery and identified by two pathologists at Hunan Cancer Hospital. Tissues were routinely embedded in paraffin, followed by slicing and dewaxing. After antigen retrieval in boiled solution of sodium citrate (0.01 M and pH = 6.0), slices were immersed in 2% H2O2 for 30 min, blocked with normal goat serum for 30 min, sequentially incubated with primary antibodies at 4°C overnight and second antibodies for 2 h at room temperature, and stained with DAB (BOSTER, Wuhan, China) for 5 min. Then, slices were sequentially counterstained with hematoxylin (BOSTER) for 1 min at room temperature and treated with PBS for 15 min at room temperature. The stained slices were sealed with neutral resin and viewed under inverted microscopy.

The following antibodies including mouse anti-CagA (clone A-10, sc-28368, Santa Cruz), mouse anti-p53 (clone PAb 240, ab26, Abcam), and rabbit anti-PD-L1 (17952-1-AP, Proteintech), goat anti-mouse IgG (HRP-linked) (AP124P, Merck Millipore), and goat anti-rabbit IgG (HRP-linked) (AP132P, Merck Millipore) were used for IHC staining of human GC tissue specimens, and antibodies rabbit anti-PD-L1 (17952-1-AP, Proteintech), rabbit anti-CD8 (ab4055, Abcam), goat anti-mouse IgG (HRP-linked) (AP124P, Merck Millipore), and goat anti-rabbit IgG (HRP-linked) (AP132P, Merck Millipore) were used for IHC staining of mouse tissue specimens according to manufacturer's instructions. Three fields per slices were analyzed, and one-fifth of cases were scored by two observers. CagA-negative (−) group was defined as no or mild staining with less than 10% positive rate of IHC staining, while other slices were defined as CagA-positive (+) group.[51] p53-negative group was defined as less than 5% positive rate of IHC staining, while other slices were defined as p53-positive group. For PD-L1 level, both membranous and cytoplasmic staining were evaluated based on the extent of IHC staining (the percentages of positive cells were scored: 0, negative or <5% staining; 1, 6–25% staining; 2, 26–50% staining; and 3, >50% staining) and the intensity of IHC staining (0, no staining; 1, weak staining; 2, moderate staining; and 3, strong staining). A total score of more than 3 was defined as positive expression of PD-L1 protein.[52]

Isolation and characterization of exosomes

Exosomes from the plasma of GC patients were isolated using ExoQuick Plasma Prep with Thrombin (System Biosciences) according to manufacturer's instructions. In brief, 500 μL of plasma and 250 μL of thrombin were mixed and incubated for 15 min, which were centrifuged at 1 000 × g for 5 min at room temperature. The collected supernatant by centrifuging was mixed with 190 μL of ExoQuick solution and incubated at 4°C for 30 min. Then, the mixture was centrifuged at 4°C and 1 500 × g for 30 min, and the obtained pellets were resuspended in 200 μL of ice-cold PBS.

Exosomes derived from the supernatants of cultured GC cells were isolated by ultracentrifugation method according to previous research methods.[53] In brief, the supernatants were sequentially centrifuged at 4°C and 2 000 × g for 20 min and centrifuged at 4°C and 10 000 × g for 30 min. The supernatants were then ultracentrifuged at 4°C and 100 000 × g for 70 min. Pellets left on the bottoms of tubes were resuspended by PBS, which were ultracentrifuged at 4°C and 100 000 × g for 70 min again. The pellets left on the bottom of the tubes were the isolated exosomes, which were resuspended in 100 μL of PBS and collected for follow-up experiments.

Western blot was conducted to examine the expression of specific protein markers of exosomes. The size and number of exosomes were identified by nanoparticle tracer analysis (NTA) on a Nanosight NS300 analyzer (Malvern Instruments Ltd, UK), and the morphology of exosomes was photographed by TEM using JEM-3010 electron microscope (JEOL, Japan). Besides, exosomal PD-L1 protein was examined by Western blot, and the relative density of exosomal PD-L1 protein was calculated using ImageJ software (National Institutes of Health, USA).

Isolation of $CD8^+$ T cells

Peripheral blood mononuclear cells (PBMCs) of human were freshly isolated from the peripheral blood of healthy individuals using Lympholyte-H (Cedarlane, Canada) according to the manufacturer's instruction. Then, $CD8^+$ T cells were purified from PBMCs using the MojoSort Human CD8 Naive T cell Isolation Kit (Biolegend, USA) based on the negative sorting method according to the manufacturer's instruction. The isolated human $CD8^+$ T cells were cultivated in RPMI 1640 medium supplemented with 10% (v/v) FBS and penicillin-streptomycin.

Mouse $CD8^+$ T cells were isolated from spleens of 615 mouse. Spleen of 615 mouse was cut into small pieces of about 1 mm^3, digested using 0.05–0.10% Collagenase II (ThermoFisher Scientific) at 37°C for 30 min, and filtered using 70 μm cell sieves to obtain single cell suspensions. Next, mouse spleen lymphocytes were isolated from the suspension of single cells using Lympholyte-M (Cedarlane) according to the manufacturer's instruction, and $CD8^+$ T cells were isolated from mouse spleen lymphocytes using the MojoSort Mouse CD8 Naive T cell Isolation Kit (Biolegend) based on negative sorting method according to the manufacturer's instruction. The isolated mouse $CD8^+$ T cells were cultivated in RPMI 1640 medium supplemented with 10% (v/v) FBS and penicillin-streptomycin.

Treatment of $CD8^+$ T cells with exosomes

To block exosomal PD-L1, 200 μg of human- or mouse-derived exosomes were incubated with anti-PD-L1 antibodies (10 μg/mL, BE0285 for human and BE0101 for mouse, BioXCell, USA) or isotype IgGs (10 μg/mL, BE0086 for human and BE0090 for mouse, BioXCell) in 100 μL PBS, respectively. Then, the treated exosomes were washed with 30 mL of ice-cold PBS and pelleted by ultracentrifugation to remove the unbound antibodies. Purified $CD8^+$ T cells (2×10^5 cells per well in a 96-well plate) were stimulated with anti-CD3 (2 μg/mL, 317353 for human and 100339 for mouse, BioLegend) and anti-CD28 (2 μg/mL, 377803 for human and 102115 for mouse, BioLegend) antibodies for 24 h. Then, exosomes at final concentration of 25 μg/mL (human) and 100 μg/mL (mouse) derived from Flag-*CagA* or Flag-vector transfected GC cells that treated with IgG or anti-PD-L1 antibody were added into culture medium of $CD8^+$ T cells and continuously cultured for 48 h in the presence of anti-CD3/CD28 antibodies. Proliferation of $CD8^+$ T cells was examined using CCK8 (Dojindo, Japan) and the levels of secreted cytokines (IFN-γ, TNF-α, and IL-2) in the supernatants of human $CD8^+$ T cells were measured by ELISA according to the instructions of commercial kits (Sino Biological, China). The details of ELISA kits are presented in key resources table.

Tumor xenograft

To observe the influence of exosomal PD-L1 on tumor growth *in vivo*, 5×10^6 MFC cells were administered to a 615 mouse by subcutaneous injection. After the formation of visible tumors (10 days post cell injection), mice were randomly divided into two groups (n = 5 each), and 100 μg of exosomes derived from Flag-*CagA* or Flag-vector transfected MFC cells in 100 μL of PBS were administered into mice every three days by tail vein injection. Mice were euthanized before tumors reached 1.50 cm in the longest dimension, and tumors were collected for further research. Tumor volume was calculated according to the formula: tumor volume (mm^3) = 0.5 × length × width.^{2} Tumor specimens were fixed in 4% paraformaldehyde, embedded in paraffin, sliced, and examined by IHC staining.

QUANTIFICATION AND STATISTICAL ANALYSIS

Data were statistically processed using SPSS 22.0 software (IBM Corporation, USA), and figures were drawn using GraphPad Prism 8.0 software (GraphPad, USA). The relationship between the positive expression or protein levels of CagA, P53, PD-L1, exosomal PD-L1 and clinicopathological characteristics was analyzed by the Chi-square analysis (two-sided). Pearson (r) or Spearman (ρ) correlation test was applied to analyze the correlations among the positive rates of CagA, P53, and PD-L1 proteins and the protein level of exosomal PD-L1. Kaplan–Meier analysis (log rank test) was used to determine the influence of PD-L1 level on overall prognosis, and the high and low levels of exosomal PD-L1 were determined according to the median value. Two-sided Student's *t* tests were performed to compare the significance of differences between two groups, and one-way ANOVA with the Tukey-Kramer or Games-Howell post hoc test was used to compare the significance of differences among multiple groups. Data are presented as mean ± SD with at least three biological replicates. Significance levels were set to $*p < 0.05$, $**p < 0.01$, $***p < 0.001$, or nonsignificant (ns).